We are IntechOpen,
the world's leading publisher of
Open Access books
Built by scientists, for scientists

6,300
Open access books available

170,000
International authors and editors

185M
Downloads

154
Countries delivered to

Our authors are among the

TOP 1%
most cited scientists

12.2%
Contributors from top 500 universities

CLARIVATE ANALYTICS
BOOK CITATION INDEX
INDEXED

WEB OF SCIENCE™

Selection of our books indexed in the Book Citation Index
in Web of Science™ Core Collection (BKCI)

Interested in publishing with us?
Contact book.department@intechopen.com

Numbers displayed above are based on latest data collected.
For more information visit www.intechopen.com

Chapter

Terfenol-D Layer in a Functionally Graded Pipe Transporting Fluid for Free Vibration

Mukund A. Patil and Ravikiran Kadoli

Abstract

Knowledge of natural frequency of pipeline conveying fluid has relevance to designer to avoid failure of pipeline due to resonance. The damping characteristics of pipe material can be increased by using smart materials like magnetostrictive namely, TERFENOL-D. The objective of the present chapter is to investigate vibration and instability characteristics of functionally graded Terfenol-D layered fluid conveying pipe utilizing Terfenol-D layer as an actuator. First, the divergence of fluid conveying pipe is investigated without feedback control gain and thermal loading. Subsequently, the eigenvalue diagrams are studied to examine methodically the vibrational characteristics and possible flutter and bifurcation instabilities eventuate in different vibrational modes. Actuation of Terfenol-D layer shows improved stability condition of fluid conveying pipe with variation in feedback control gain and thermal loading. Differential quadrature and differential transform procedures are used to solve equation of motion of the problem derived based on Euler-Bernoulli beam theory. Finally, the effects of important parameters including the feedback control gain, thermal loading, inner radius of pipe and density of fluid on vibration behavior of fluid conveying pipe, are explored and presented in numerical results.

Keywords: control gain, isothermal load, flutter, bifurcation instability, differential quadrature and differential transform method

1. Introduction

Composite fluid-conveying pipes have become a practicable substitute to metallic pipes in several engineering applications such as oil and gas transport lines, hydraulic and pneumatic systems, thermal power plants, heat transfer equipment, petroleum and chemical process industries, underground refueling pipelines in airports, hospitals, medical devices, municipal sewage and drainage, corporation water supply and many more. Divergence and flutter instabilities are illustrious in fluid-conveying pipe due to fluid–structure interaction. One type of instability encountered in cantilever fluid-conveying pipes is called bifurcation, when the imaginary portion of the

complex frequency disappears and the real portion splits into two branches. Fundamental concepts and early development in fluid structure interaction of fluid conveying pipes have been complied and studied by [1] systematically. A few more specialized topics are briefly discussed and well documented in Ref. [2–4]. Remarkable contributions in the area of fluid-conveying pipe vibrations also include the works of Chen [5].

In the meantime, performing a review on literature, it can be seen that a few studies have been carried out in the several field of vibrations such as in-depth nonlinear dynamics [6–10], vibration control [11–18], microtubes or nanotubes in microfluidic devices [19–22], and pipes using functionally graded materials [23–26].

The pseudo excitation method in conjunction with the complex mode superposition method was deduced to solve dynamic equation of Timoshenko pipeline conveying fluid [6]. The post-buckling and closed-form solutions to nonlinear frequency and response [8] of a FG fluid-conveying pipe have been investigated using analytical homotopy analysis method. Natural frequencies and critical flow velocities has been obtained for free vibration problem of pipes conveying fluid with several typical boundary conditions using DTM [11]. Dynamics and pull-in instability of pipes conveying fuid with nonlinear magnetic force have been investigated by [13], for clamped-clamped and clamped-free boundary conditions. The conclusion of investigation is that, location of magnets has a great impact on the static deflection and stability of the pipe. Wavelet based FEM has been used to examine the effect of internal surface damage [14] on free vibration behavior of fluid-conveying pipe. The natural frequencies of pipe conveying fluid has been determined by [15], using Muller's bisection method.

Failure due to filament wound with consideration of production process inconsistencies have been assessed by Rafiee et al. [16]. Vibration and instability response of magnetostrictive sandwich cantilever fluid-conveying micro-pipes is investigated utilizing smart magnetostrictive layers as actuators by [18].

Nonlinear vibration of a carbon nanotube conveying fluid with piezoelectric layer lying on Winkler-Pasternak foundation under the influence of thermal effect [21] and magnetic field [22] have been investigated using Galerkin and multiple scale method. The in-plane free vibration frequency of a zirconia-aluminum functionally graded curved pipe conveying fluid have been explored by the complex mode method [23]. The effect of axial variations of elastic modulus and density on dynamical behavior of an axially functionally graded cantilevered pipe conveying fluid has been analyzed by [24]. Dai et al. [25] studied the thermo-elastic vibration of axially functionally graded pipe conveying fluid considering temperature changes. Heshmati [26] studied the stability and vibration behaviors of functionally graded pipes conveying fluid considering the the effect of eccentricity imperfection induced by improper manufacturing processes. Xu Liang et al. [27] have used differential quadrature method (DQM) and the Laplace transform and its inverse, to analyze the dynamic behavior of a fluid-conveying pipe with different pipe boundary conditions. Huang Yi-min et al. [28] used the separation of variables method and the derived method from Ferrari's method to decouple the the natural frequency and the critical flow velocity equations of fluid-conveying pipe with both ends supported. Planar and spatial curved fluid-conveying pipe [29] have been investigated for their free vibration behavior with Timoshenko beam model and B-spline function used as the shape function in Galerkin method.

There are few investigations in the literature on fluid-conveying pipes containing Terfenol-D layers. Certainly, a study on the mechanical behavior of functionally graded Terfenol-D layered fluid conveying pipe will contribute to the understanding

for future design engineers, hence an attempt on the vibration and stability of functionally graded Terfenol-D layered fluid conveying pipe. Inherent features of the Terfenol-D layer to regulate the vibration instabilities and critical flow velocity of a FGMT pipe are attempted numerically. Terfenol-D is a popular magnetostrictive material exhibiting force output for a corresponding magnetic field input and produces magnetic field for mechanical force as an input. Every term in Terfenol-D has a meaning (see **Figure 1**), for example, Ter means Terbium, Fe signifies chemical symbol for iron, Nol stands for Naval Ordnance Laboratory, and D stands for Dysprosium [30]. Terfenol-D has numerous distinguish characteristics, including a high electromechanical coupling coefficient (0.73), a high magnetostrictive strain (800–1600 ppm), a fast response, a high energy density, and a large output force. The total stiffness of the pipe is affected by actuation of the Terfenol-D layer due to the creation of tensile forces with a change in feedback control gain and temperature change in the fluid-conveying pipe. The governing equation of motion for FGMT fluid-conveying pipe is derived based on Euler-Bernoulli's theory. Differential quadrature and differential transform approaches are used to obtain the frequency of boundary value problem. Critical velocities of the FGMT pipe are also determined for various boundary conditions, feedback control gain, and thermal loading. Validation of frequencies and critical velocities is accomplished using accessible analytical relations.

2. Functionally graded fluid conveying pipe

Powder metallurgy is considered as manufacturing process for present functionally graded Terfenol-D layered fluid-conveying pipe. The functioanlly graded pipe is assumed to compose of aluminum (as metallic) and aluminum oxide (as ceramic). In between the graded composition of aluminum and aluminum oxide Terfenol-D layer is included. The material properties, volume fraction and expression for calculation of properties is given in [31]. **Figure 2** shows the layout of FGMT fluid-conveying pipe.

2.1 Derivation of governing equation

Considering the FGMT fluid-conveying pipe as an Euler-Bernoulli beam, the equation for the motion of the pipe can be derived using Hamilton's principle. The
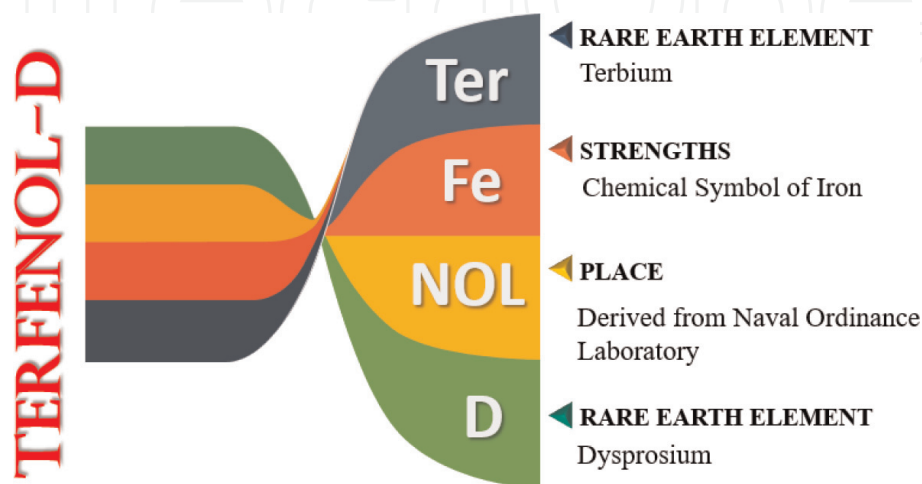
Figure 1.
Schematic for meaning of Terfenol-D.
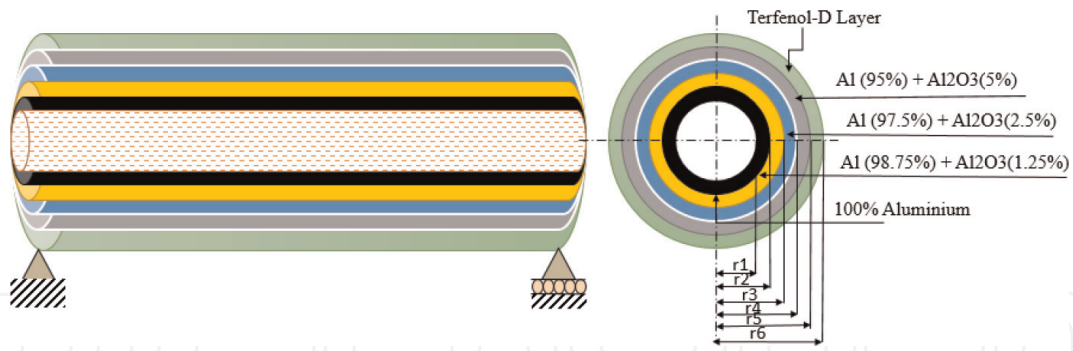
Figure 2.
Physical model of simply supported FGMT fluid-conveying pipe.

kinetic energy of the internal fluid is appended to the kinetic energy of the pipe to obtain total kinetic energy of FGMT pipe, and is described by the equation

$$J = J_p + J_f \tag{1}$$

Where, J_p and J_f signify the kinetic energy of the composite FGMT fluid-conveying pipe and the kinetic energy of the fluid flowing through the pipe, respectively. The elements of kinetic energy (J) as defined in Eq.(1) can be expressed as:

$$J_p = \frac{1}{2} \int_0^l m_p \left(\frac{\partial w}{\partial t} \right)^2 dx \tag{2}$$

$$J_f = \frac{1}{2} \int_0^l m_f \left(\left(v \frac{\partial w}{\partial x} + \frac{\partial w}{\partial t} \right)^2 + v^2 \right) dx \tag{3}$$

Where, w symbolize for the displacement in the vertical direction, v symbolize for the fluid velocity, The flow of liquid, water, oil, and similar liquid flowing through the pipe are assumed to have a flat velocity profile at every section of the flow (i.e. popularly called as plug flow). m_p and m_f respectively denote the mass per unit length of the pipe and the internal fluid. The strain energy U of the fluid-conveying pipe can be defined as:

$$U = \frac{1}{2} \int_0^l E_p I_p \left(\frac{\partial^2 w}{\partial x^2} \right)^2 dx \tag{4}$$

Where $E_p I_p$ is the flexural rigidity of the FGMT fluid-conveying pipe. Constitutive relation for a magnetostrictive beam type structure [32] could be written as:

$$\sigma_{xx}^T = C_{11} \epsilon_{xx} - e_{31} H_z \tag{5}$$

where σ_{xx}^T, ϵ_{xx} signifies axial stress and strain of the Terfenol-D layer. In addition, C_{11} and e_{31} are elastic stiffness coefficient and magnetostrictive constant, respectively. The subscript 31 indicates that, the magnetic field is applied in the 3(z) direction and mechanical response obtained in the 1(x) direction. The strength of the magnetic field H_z may now be stated as follows.

$$H_z = k_c C(t) \frac{\partial w}{\partial t} \tag{6}$$

Where, k_c, $C(t)$ and $\frac{\partial w}{\partial t}$ denotes the coil constant, feedback control gain and transverse displacement of fluid conveying pipe with respect to time, respectively. The strain energy of the Terfenol-D layer is given as:

$$U_T = \int_0^l \int_A \sigma_{xx}^T \epsilon_{xx} \mathrm{d}A dx \qquad (7)$$

Also, the axial moment produced by Terfenol-D layer is,

$$M_{xx} = \int_A \sigma_{xx}^T z \mathrm{d}A \qquad (8)$$

Applying the Hamilton's principle, one can write the functional of FGMT pipe as,

$$\int_{t_1}^{t_2} \delta(J - U - U_T) \mathrm{d}t + \int_{t_1}^{t_2} \delta W_{force} \mathrm{d}t = 0 \qquad (9)$$

Where, J is the total kinetic energy of the system; U is the deformation energy of the system; W_{force} denotes the work of the non-conservative force. Therefore, the equation of motion for the free vibration of FGMT composite pipe conveying fluid can be written as:

$$\underbrace{E_p I_p \frac{\partial^4 w}{\partial x^4}}_{\text{Elastic}} + \underbrace{m_f v^2 \frac{\partial^2 w}{\partial x^2}}_{\text{Centrifugal}} + \underbrace{2 m_f v \frac{\partial^2 w}{\partial x \partial t}}_{\text{Coriolis}} + \underbrace{\varepsilon \frac{\partial^2 w}{\partial x \partial t}}_{\text{Magnetostrictive Moment}} + \underbrace{(m_p + m_f) \frac{\partial^2 w}{\partial t^2}}_{\text{Inertia}} = 0 \quad (10)$$

The governing equation for FGMT fluid-conveying pipe with thermal loading making use of Ref. [33] can be obtained as:

$$E_p I_p \frac{\partial^4 w}{\partial x^4} + \left(m_f v^2 + A\gamma(\Delta T)\right) \frac{\partial^2 w}{\partial x^2} + 2 m_f v \frac{\partial^2 w}{\partial x \partial t} + \varepsilon \frac{\partial^2 w}{\partial x \partial t} + (m_p + m_f) \frac{\partial^2 w}{\partial t^2} = 0 \quad (11)$$

Where,

$$m_p = \sum_{j=1}^n \pi \rho_j \left(r_{j+1}^2 - r_j^2\right) \qquad (12)$$

$$E_p I_p = A_{11} r^3 - D_{11} r \qquad r = \frac{d_o + d_i}{4} \qquad (13)$$

$$A_{11} = \sum_{j=1}^n Q_{11} \left(r_{j+1} - r_j\right) \qquad (14)$$

$$D_{11} = \frac{1}{3} \sum_{j=1}^n Q_{11} \left(r_{j+1}^3 - r_j^3\right) \qquad (15)$$

$$\varepsilon = e_{31} k_c C(t) \left(r_{j+1}^2 - r_j^2\right) \qquad (16)$$

$$\gamma(\Delta T) = E\alpha\Delta T \qquad (17)$$

Where, α indicates the thermal expansion coefficient of the fluid conveying pipe material, ΔT is the temperature change in the layers, E is the Young's modulus of the fluid conveying pipe and $\gamma(\Delta T)$ symbolize the linear elastic stress–temperature coefficient.

3. Transformation of PDE into a sets of ODEs

Authors used the differential quadrature method to solve the free vibration equation of FGMT fluid-conveying pipe as given in Eq. (9). Here, the Eq. (9) is transformed into sets of ordinary differential equations. The standard eigenvalue form [34, 35] of the Eq. (9) can be obtained by assuming:

$$w_0 = W_0 e^{\Lambda t} \tag{18}$$

W_0 is the mode shape of transverse motion and Λ is the frequency of the FGMT fluid-conveying pipe. Substitute the Eq. (12) in Eq. (9), accordingly Eq. (9) re-reads as follows:

$$E_p I_p \frac{\partial^4}{\partial x^4}\left(W_0 e^{\Lambda t}\right) + m_f v^2 \frac{\partial^2}{\partial x^2}\left(W_0 e^{\Lambda t}\right) + 2m_f v \frac{\partial}{\partial x}\left(\frac{\partial}{\partial t} W_0 e^{\Lambda t}\right) + \epsilon \frac{\partial}{\partial x}\left(\frac{\partial}{\partial t} W_0 e^{\Lambda t}\right)$$

$$+ (m_p + m_f)\frac{\partial^2}{\partial t^2}\left(W_0 e^{\Lambda t}\right) = 0$$

$$\tag{19}$$

$$\left(E_p I_p \frac{d^4 W_0}{dx^4} e^{\Lambda t}\right) + \left(m_f v^2 \frac{d^2 W_0}{dx^2} e^{\Lambda t}\right) + \left(2m_f v \frac{dW_0}{dx} e^{\Lambda t}\right)\Lambda + \left(\epsilon \frac{dW_0}{dx} e^{\Lambda t}\right)\Lambda \tag{20}$$

$$+ \left((m_p + m_f) W_0 e^{\Lambda t}\right)\Lambda^2 = 0$$

$$\left(E_p I_p \frac{d^4 W_0}{dx^4}\right) + \left(m_f v^2 \frac{d^2 W_0}{dx^2}\right) + \left((2m_f v^2 + \epsilon)\frac{dW_0}{dx}\right)\Lambda + \left((m_p + m_f) W_0\right)\Lambda^2 = 0$$

$$\tag{21}$$

Now, substitute the analog form of differential quadrature for respective derivative (first, second, third and fourth) such as:

$$\frac{d^4 W_0}{dx^4} = \sum_{j=1}^{N} A_{ij}^{(4)} W_j, \qquad \frac{d^2 W_0}{dx^2} = \sum_{j=1}^{N} A_{ij}^{(2)} W_j, \qquad \frac{dW_0}{dx} = \sum_{j=1}^{N} A_{ij}^{(1)} W_j \tag{22}$$

Now, Eq.15 becomes,

$$E_p I_p \sum_{j=1}^{N} A_{ij}^{(4)} W_j + m_f v^2 \sum_{j=1}^{N} A_{ij}^{(2)} W_j + \left((2m_f v^2 + \varepsilon)\sum_{j=1}^{N} A_{ij}^{(1)} W_j\right)\Lambda + \left((m_p + m_f) W_i\right)\Lambda^2$$

$$= 0$$

$$\tag{23}$$

Now separate the terms associated with Λ and Λ^2 to prepare the damping and mass matrices, respectively as shown in Eq. 18.

$$\{-[M]\Lambda^2\}\{d\} + \{[\Gamma]\Lambda\}\{d\} + [K]\{d\} = 0 \tag{24}$$

Where,

$$[\Gamma] = [C_{dd}] - [C_{db}][S_{bb}]^{-1}[S_{bd}] \tag{25}$$

$$[K] = [S_{dd}] - [S_{db}][S_{bb}]^{-1}[S_{bd}] \tag{26}$$

Where, C_{dd} and C_{db} are the damping sub matrices which includes the domain-domain and domain-boundary elements of damping. Similarly, S_{bb}, S_{bd}, S_{db} and S_{dd} are the stiffness sub matrices which includes the boundary-boundary, boundary-domain, domain-boundary and domain-domain elements, respectively. The standard form of eigenvalue can be obtained from Eq. (18) as:

$$\left\{ \begin{bmatrix} 0 & I \\ \Gamma & K \end{bmatrix} - \begin{bmatrix} I & 0 \\ 0 & M \end{bmatrix} \Lambda \right\} \begin{Bmatrix} d \\ \Lambda d \end{Bmatrix} = 0 \tag{27}$$

Where I, $[K]$, $[\Gamma]$ and $[M]$ denote the identity, structural stiffness, damping and mass matrix, respectively. One can obtain the two sets of eigenvalues. The eigenvalue obtained can be written as $\Lambda = -\alpha \pm i\omega_d$.

4. Application of differential transform method to FGMT fluid-conveying pipe

Differential transform technique (DTM) may be used to solve integral equations, ordinary partial differential equations, and differential equation systems. Using this approach, a polynomial solution to differential equations may be derived analytically. For large orders, the Taylor series approach is computationally time-consuming. This method is appropriate for linear and nonlinear ODEs since it does not need linearization, discretization, or perturbation. It is also possible to significantly reduce the amount of computing labour required while still precisely delivering the series solution and rapidly converging. The DTM has several disadvantages, though. Using the DTM, a truncated series solution may be obtained. This truncated solution does not display the actual behavior of the problem, but in the vast majority of situations it offers a good approximation of the actual solution in a relatively limited area. Solutions are expressed as convergent series with components that may be readily computed using the differential transform technique. The linear equation of motion for free vibration of FGMT fluid-conveying pipe is given by,

$$\left(E_p I_p \frac{d^4 W_0}{dx^4} \right) + \left(m_f v^2 \frac{d^2 W_0}{dx^2} \right) + \left((2m_f v^2 + \varepsilon) \frac{dW_0}{dx} \right) \Lambda + ((m_p + m_f) W_0) \Lambda^2 = 0 \tag{28}$$

The differential transformation form of Eq. (22) can be written as

$$E_p I_p ((i+1)(i+2)(i+3)(i+4)W(i+4)) + m_f v^2 ((i+1)(i+2)W(i+2)) \\ + (2m_f v^2 + \varepsilon)((i+1)W(i+1)) + (m_p + m_f)W(i) = 0 \tag{29}$$

	x = 0		x = 1
Original Form	**DTM Form**	**Original Form**	**DTM Form**
$w(0)=0$	$W(0)=0$	$w(1)=0$	$\sum_{i=0}^{N} W(i)=0$
$\frac{dw}{dx}(0)=0$	$W(1)=0$	$\frac{dw}{dx}(1)=0$	$\sum_{i=0}^{N} iW(i)=0$
$\frac{d^2w}{dx^2}(0)=0$	$W(2)=0$	$\frac{d^2w}{dx^2}(1)=0$	$\sum_{i=0}^{N} i(i-1)W(i)=0$
$\frac{d^3w}{dx^3}(0)=0$	$W(3)=0$	$\frac{d^3w}{dx^3}(1)=0$	$\sum_{i=0}^{N} i(i-1)(i-2)W(i)=0$

Table 1.
Transformed form of boundary condition for differential transform method.

Rearranging Eq. (23), one will get a simple recurrence relation as:

$$W(i+4) = -\frac{\left(m_f v^2 (i+1)(i+2)W(i+2) + \left(2m_f v^2 + \varepsilon\right)(i+1)W(i+1) + \left(m_p + m_f\right)W(i)\right)}{E_p I_p (i+1)(i+2)(i+3)(i+4)}$$

(30)

Similarly, analogous form of original boundary conditions for the differential transformation can be done using **Table 1**, where $x = 0$ and $x = 1$ represents the boundary points. It can be seen that $W(i)$, $(i = 4,5,\ldots,N)$ is a linear function of $W(2)$ and $W(3)$. Thus, $W(2)$ and $W(3)$ are considered as unknown parameters and taken as $W(2) = b_1$, $W(3) = b_2$ for clamped-clamped boundary conditions. With Eq. (23), $W(i)$ can be calculated via an iterative procedure. Substituting $W(i)$ into boundary conditions at other end of FGMT pipe, the two equations (Substituting all $W(i)$ terms into boundary condition expressions) can be written as matrix form,

$$\begin{bmatrix} R_{11} & R_{12} \\ R_{21} & R_{22} \end{bmatrix} \begin{bmatrix} b_1 \\ b_2 \end{bmatrix} = 0$$

(31)

Where R_{ij} are associated with the eigenvalues ω, b_1 and b_2 are the constants and other parameters of the FGMT pipe system, corresponding to N. To obtain a non-trivial solution of Eq. (25), it is required that the determinant of the coefficient matrix vanishes, namely

$$\begin{vmatrix} R_{11} & R_{12} \\ R_{21} & R_{22} \end{vmatrix} = 0$$

(32)

Therefore, the eigenvalues ω can be computed numerically from Eq. (26). Generally, ω is a complex number.

5. Results and discussion

In the following section, the numerical results are proposed to investigate the free vibration behavior of FGMT fluid-conveying pipe subjected to control gain and thermal loading. Since there is no published research on the subject of free vibration of FGMT fluid-conveying pipes in the open literature, a differential quadrature and

differential transform approach is used to conduct a condensed analysis of the current study. The imaginary component ($\mathfrak{Im}$) of the complex frequency [$\Omega = \mathfrak{Re}(\Omega) \pm \mathfrak{Im}(\Omega)$] denotes the energy stored in either mass or strain energy in the fluid conveying pipe. The accumulated strain energy is linked to the failure behavior of the fluid conveying pipe. Furthermore, the real element ($\mathfrak{Re}$) of the complex frequency represents damping and the energy that will be transformed to heat or other energy by friction or other molecular actions.

5.1 Validation of present study

The current MATLAB code for the differential quadrature and transform technique is validated using Ref. [28], as shown in **Table 2**. The validation for FGMT fluid conveying pipe is also given by the author in Ref. [36]. Furthermore, the solution obtained using the differential quadrature approach corresponds well with the solution acquired using the differential transform method.

It has been identified that, the differential transform method requires the 58 number of terms to get the converged solution whereas 19 grid points used to obtain the convergence solutions shown. The natural frequencies of pipes conveying fluid depend on the fluid velocity v. The physical parameters of FGMT fluid-conveying pipe are calculated as: $m_p = 1.0670 \text{ kg} - \text{m}$, $m_f = 0.23562 \text{ kg} - \text{m}$, $E_p I_p = 5.1620 \text{ N} - \text{m}^2$, $L = 1 \text{ m}$. In order to calculate these physical parameters, authors have used Eq. 2.1. MATLAB software is used to create a package that performed the foregoing computations. The correctness of the results are shown by the comparison of the results of differential transform method in **Table 3** under different boundary conditions for $v = 0.5 \text{ m/s}$. The number of grid points was modified from 7 to 19 to reach the converged solution. From the **Table 3**, it can be concluded that the imaginary component of the damped frequency calculated using DQM and DTM coincides rather well.

One of the key concerns for fluid conveyance pipes to be of significant importance is stability. The natural frequencies decrease with higher flow rates for pipelines with supported ends. The system destabilizes by diverging (buckling) when the natural frequencies fall to zero, and the resulting flow velocity is known as the critical flow velocity. In the case of $v \neq 0$, **Figures 3–10** represent the natural frequencies of fluid-conveying FGMT pipe with different boundary conditions. The first three natural

| Velocity (m/s)	Method	Mode	
		λ_1	λ_2
	DQM	15.7213	31.4327
$v=0$	DTM	15.2765	31.3274
	Ref. [28]	15.71	31.42
	DQM	13.9650	30.8266
$v=10$	DTM	13.5669	30.6656
	Ref. [28]	13.97	30.83

Table 2.
Validation of simply-supported natural frequencies (rad/sec) of fluid conveying pipe (Parameters used: EI = 100 Nm², m_f = 2 kg/m, m_p = 2 kg/m and L = 1 m).

Boundary	Nodes	Mode			
		$Im(\Lambda_1)$	$Im(\Lambda_2)$	$Im(\Lambda_3)$	$Im(\Lambda_4)$
	7	18.4437	58.7726	111.9680	—
	11	18.4530	76.9717	166.6046	255.9565
S-S	15	18.4529	77.4675	175.6156	331.6998
	17	18.4529	77.4688	175.7221	313.2417
	19	18.4529	77.4688	175.7221	313.2417
DTM		18.4765	77.4445	175.6849	313.2167
	7	44.6652	94.0809	149.5829	—
	11	43.8719	120.7255	224.0424	324.0114
C-C	15	43.8700	121.9308	239.5009	435.8037
	17	43.8700	121.9365	239.7773	396.9056
	19	43.8700	121.9365	239.7780	396.9056
DTM		43.9087	122.1424	240.0518	397.2302
	7	29.5136	75.3884	133.9371	—
	11	29.8002	97.5593	196.8662	272.6251
S-C	15	29.8007	98.5000	206.4495	391.9600
	17	29.8006	98.5037	206.5287	353.8381
	19	29.8006	98.5037	206.5287	353.8381
DTM		29.8321	98.6121	206.6739	354.0290
	7	5.1817	41.1890	112.4169	—
	11	7.1259	43.1741	128.5438	207.9994
C-F	15	7.1260	43.1894	122.0607	241.8281
	17	7.1260	43.1894	121.9887	239.7690
	19	7.1260	43.1894	121.9887	239.7690
DTM		7.1487	43.5897	122.3256	240.9832

Table 3.
Convergence of imaginary component of damped frequency for different boundary conditions when $v = 5$ m/s.

frequencies of the C-F fluid-conveying FGMT pipe with $0 \leq v \leq 50$ are depicted in **Figures 3** and **4**. The critical velocity of the pipe is $v = 42$ m/s, and the third mode appears flutter instability. The findings of the differential quadrature method were utilized to plot the results presented in the **Figures 3–10**.

The first four natural frequencies of the simply supported fluid-conveying FGMT pipe with $0 \leq v \leq 50$ are plotted in **Figures 5** and **6**. The first mode appears divergence instability when the critical velocity of the FGMT pipe is $v = 15$ m/s, and Paidoussis coupled mode flutter instability appears when the critical velocity is $v = 31$. Real component ($\Re\mathfrak{e}$) of the complex frequency is almost zero during the first mode divergence instability. By increasing the flow velocity 30 m/s, the imaginary part of combination of first and second modes becomes zero, while the real part is non-zero, and the non-zero frequency and damping of first and second mode at the same values are coupled, then the system will be unstable again. This sort of instability, caused by
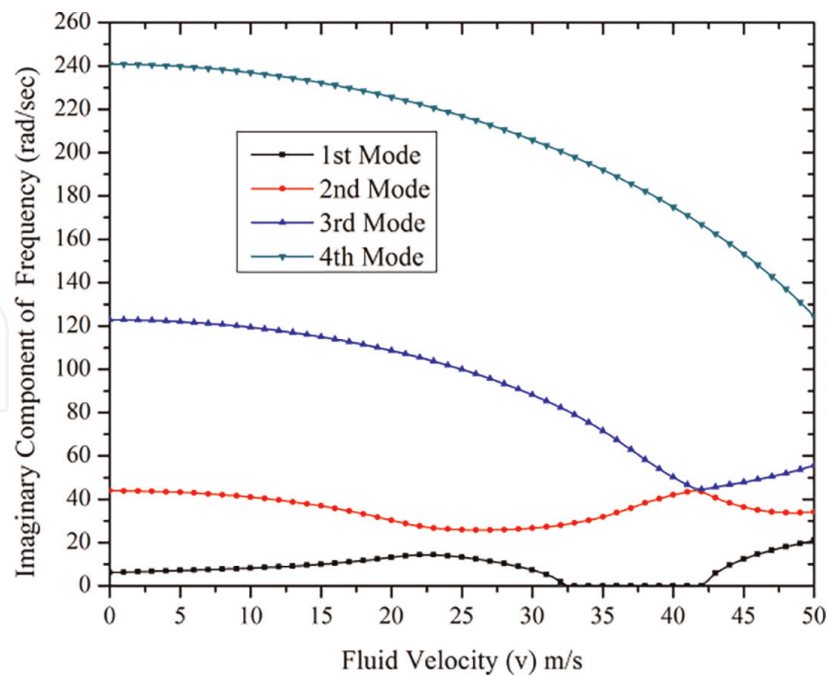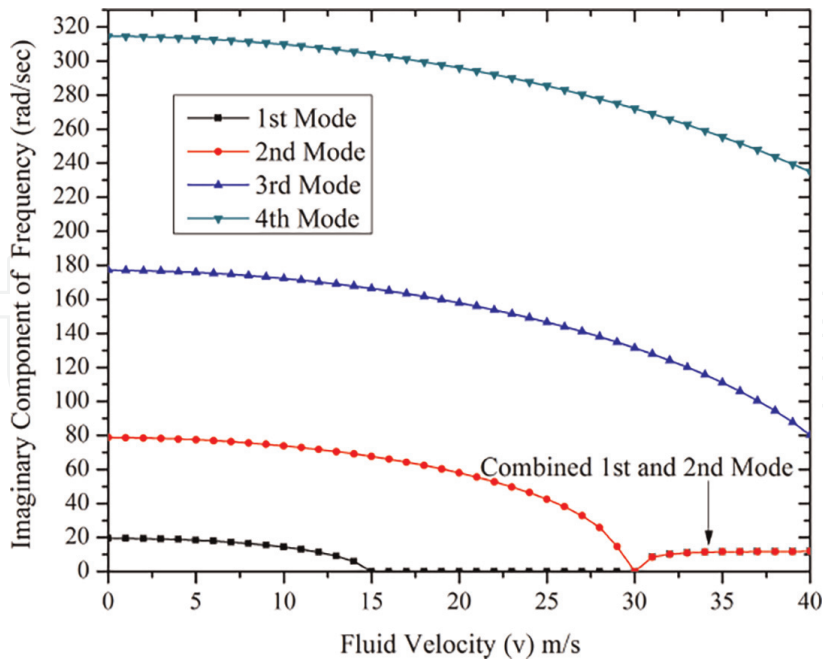
Figure 3.
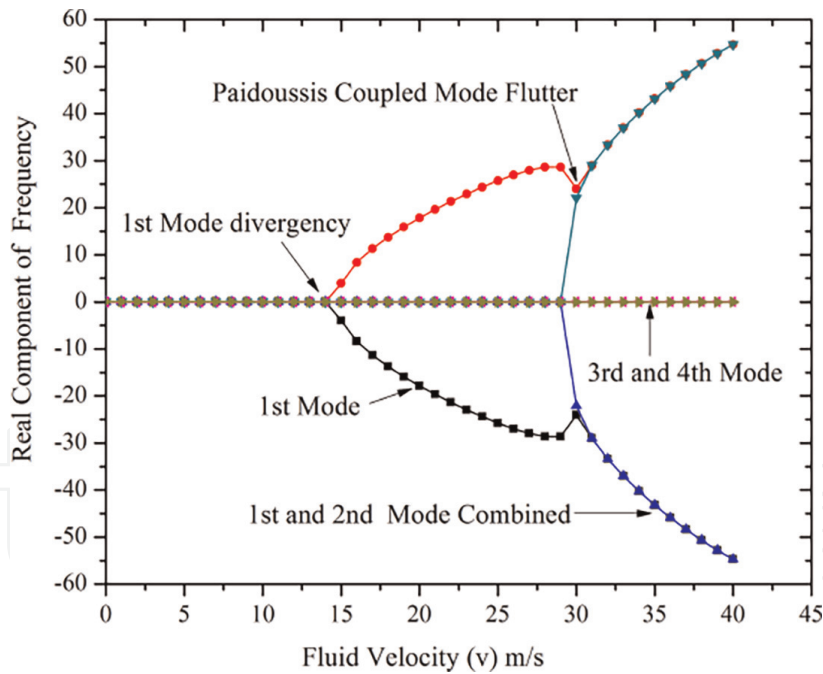*Effect of fluid velocity v on imaginary component of clamped-free damped frequency.*
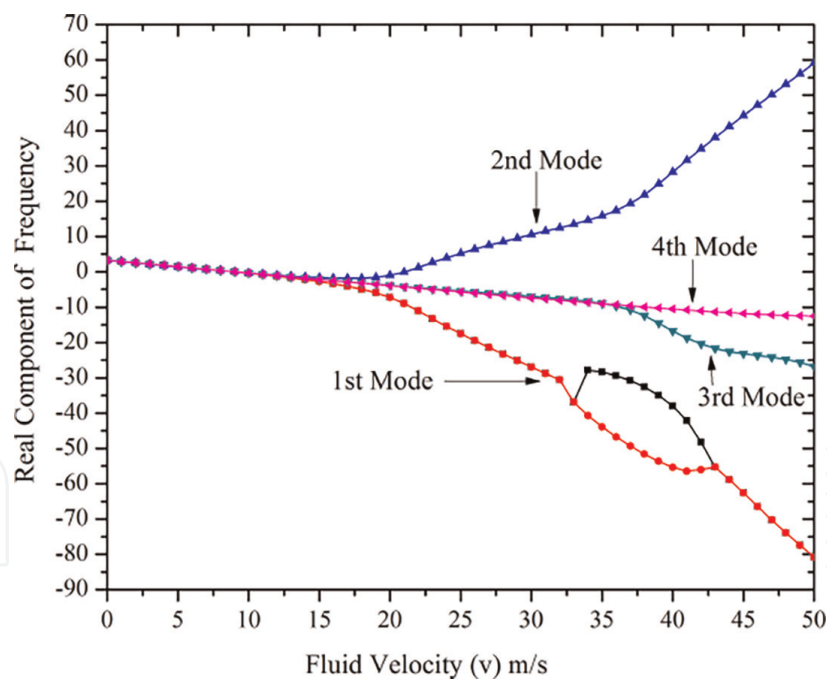
Figure 4.
Effect of fluid velocity v on real compoent of clamped-free damped frequency.

the interaction of two modes, is known as flutter instability, and its amplitude develops exponentially as a function of time.

Figures 7 and **8** shows the first four natural frequencies of the C-C fluid-conveying pipe with $0 \leq v \leq 50$. The critical velocity of the FGMT pipe is $v = 30$ m/s and 43, and corresponds to divergence instability in the first mode and couple-mode flutter instability. Bifurcation critical flow velocity is the term used to describe the flow velocity at which the bifurcation instability occurs. It should be noted that the system enters an

Figure 5.
Effect of fluid velocity v on imaginary component of simply supported damped frequency.

Figure 6.
Effect of fluid velocity v on real component of simply supported damped frequency.

over-damping mode, which prevents the FGMT pipe from vibrating, when the working fluid velocity surpasses its critical value.

Figures 9 and **10** presents the first four natural frequency of the S-C fluid-conveying FGMT pipe with $0 \leq v \leq 50$. It is obvious that the first mode appears divergence instability when fluid velocity $v = 22$ m/s, and coupled-mode flutter instability appears when fluid velocity reaches to $v = 37$ m/s. The specific critical velocities under different boundary conditions are listed in **Table 4**. The critical velocity for the
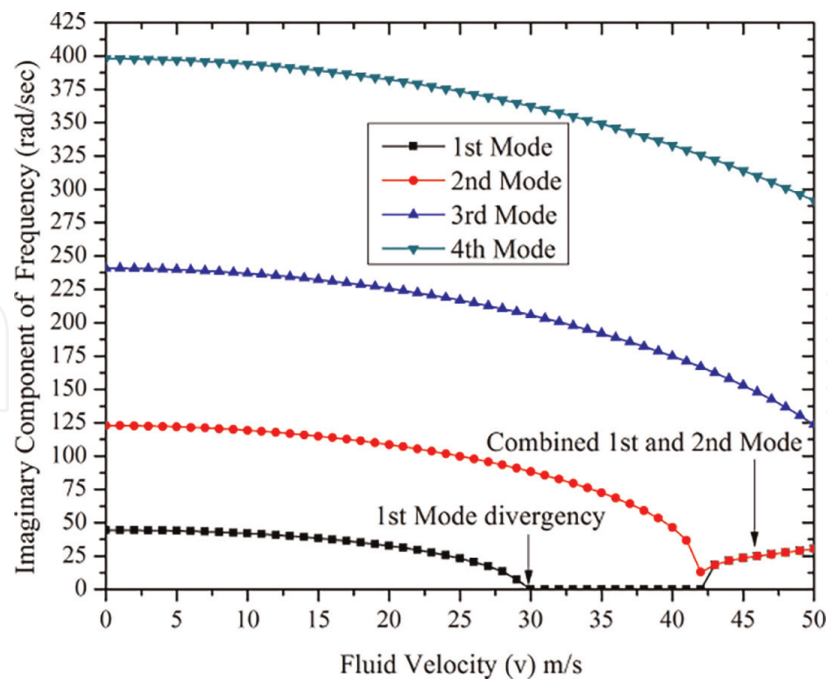
Figure 7.
Effect of fluid velocity v on imaginary component of clamped-clamped damped frequency.
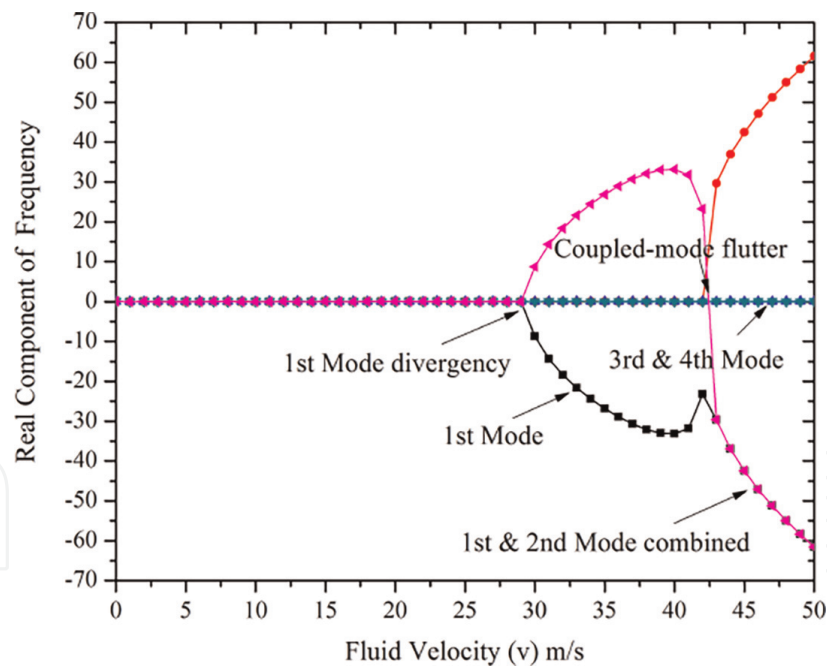
Figure 8.
Effect of fluid velocity v on real component of clamped-clamped damped frequency.
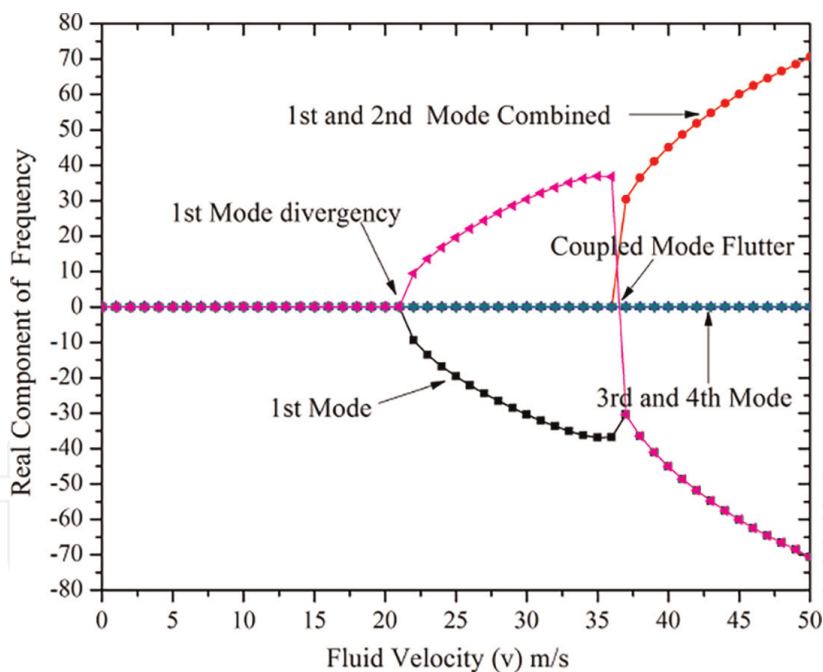
simply supported-simply supported and clamped-clamped boundary conditions are validated using Navier solution given by [37].

The relationships between the imaginary component of frequency of the FGMT pipe and the fluid density for different boundary conditions are plotted in **Figure 11**. Because the inertial and Coriolis forces were stronger with increasing fluid density, it was more simpler for the pipe to lose its stability. This led to a lower natural frequency. The changes of imaginary component of frequency with inner radius of the
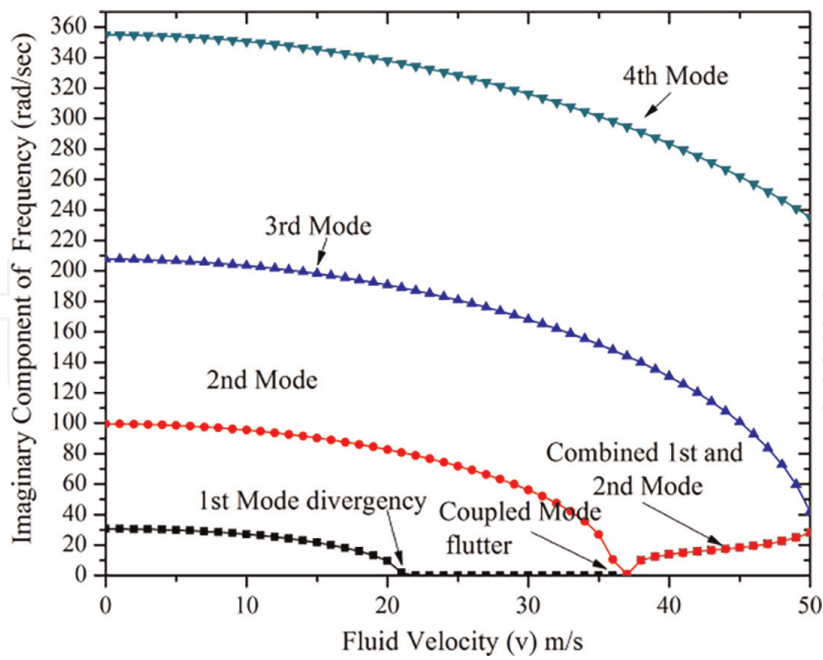
Figure 9.
*Effect of fluid velocity v on imaginary component of simply supported-clamped damped frequency.*

Figure 10.
Effect of fluid velocity v on real component of simply supported-clamped damped frequency.

FGMT pipe for different boundary conditions are shown in **Figure 12**. For very small values of the inner radius, an increase in the inner radius has a considerable impact on frequency; nevertheless, when the inner radius value is near to the outer radius, the frequency increases. In the boundary conditions clamped-clamped, simply supported-simply supported, and simply supported-clamped, the imaginary component of frequency drops as the feedback control gain rises. Imaginary component of the eigenvalue for a clamped-free frequency becomes zero for 3000 feedback control gain, $r = 0.005$ m and $v = 5$ m/s shown in **Figure 13**.

BC	Mode	Velocity (v)	Instability Form
S-S	1st Mode	15	Divergence
	Navier Solution [37]	15	—
	2nd Mode	30	Divergence
	1st & 2nd Combined	31	Paidoussis coupled mode flutter
C-C	1st Mode	30	Divergence
	Navier Solution [37]	30	—
	1st & 2nd Combined	43	Coupled mode flutter
C-F	3rd Mode	42	Flutter
S-C	1st Mode	22	Divergence
	1st & 2nd Combined	37	Coupled mode flutter

Table 4.
*Critical velocities for FGMT pipe with different boundary conditions.*
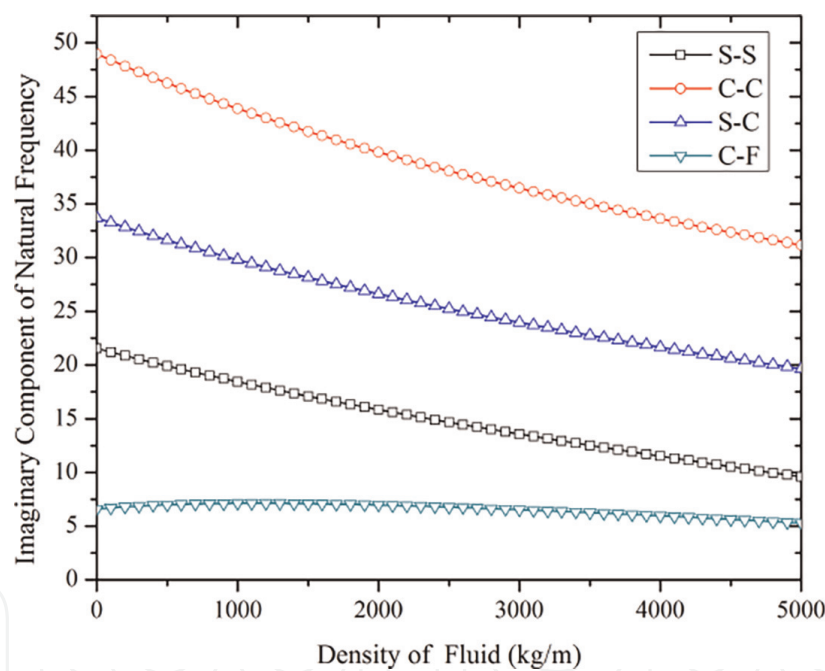
Figure 11.
Variation in fundamental natural frequency of FGMT pipe with changes in fluid density.

It is worth pointing out that the important aspect of present research work is maneuvering the use of Terfenol-D layers attached on the top FGMT fluid-conveying pipe to control the critical flow velocity and also improve the stability region. When Terfenol-D layer actuates tensile forces are generated in FGMT fluid-conveying pipe which affects the stiffness of fluid-conveying pipe. In order to evaluate this objective, **Figure 14** shows the real part ($\Re\mathfrak{e}$) of clamped-free first mode frequency with flow velocity for 0, 1000 and 1500 feedback control gain. It is observed that, 30, 28 and 9 m/s are the critical flutter velocity for 0, 1000 and 1500 feedback control gain, respectively. Therefore, one can make fluid-conveying pipe more stable by varying the feedback control gain. **Figure 15** shows the variation of analytical nonlinear
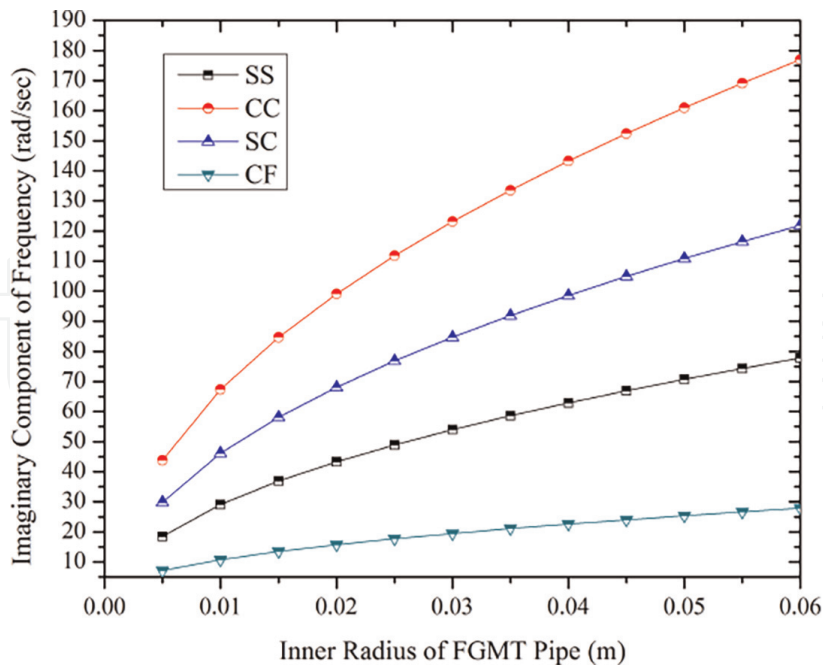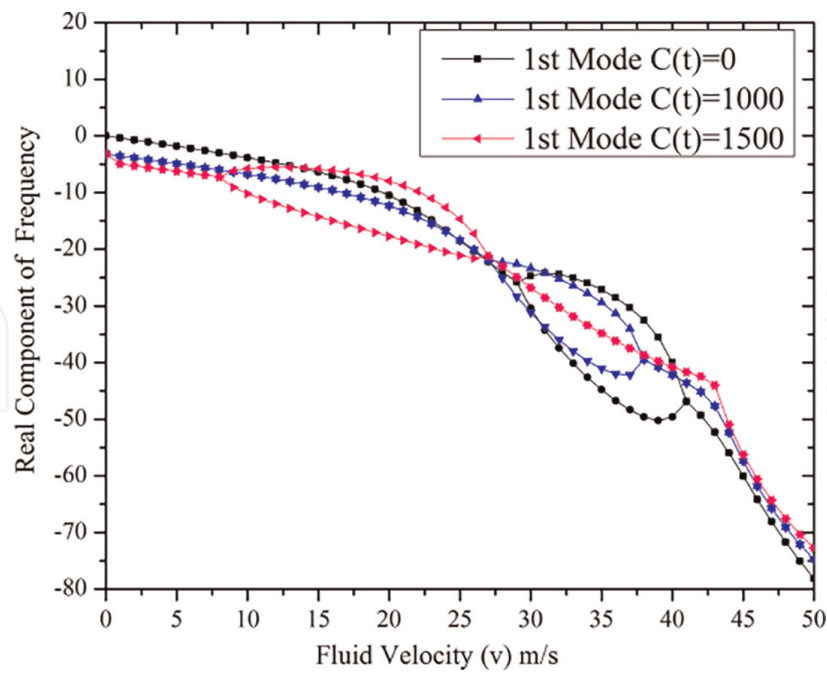
Figure 12.
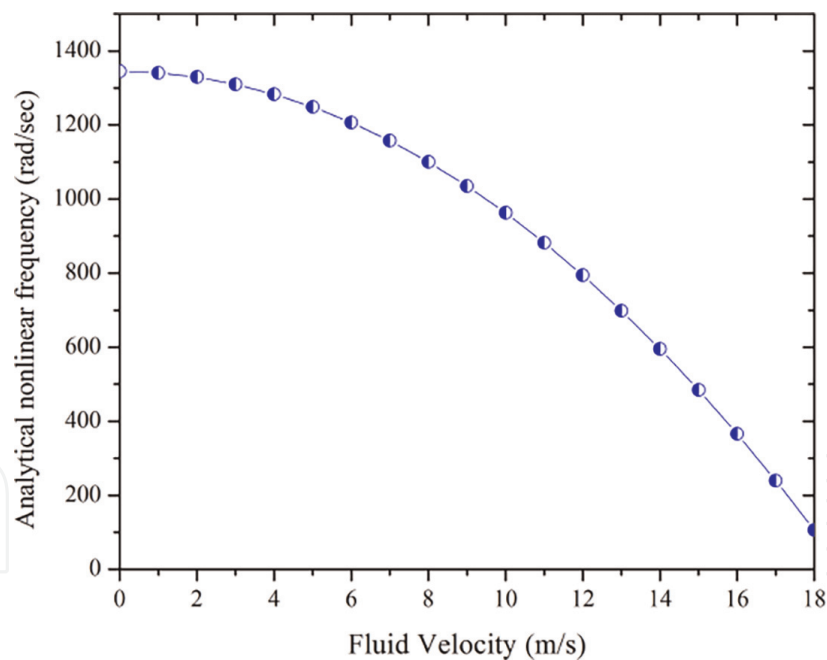*Variation of fundamental frequency with changes in inner radius of FGMT pipe for different boundary conditions.*
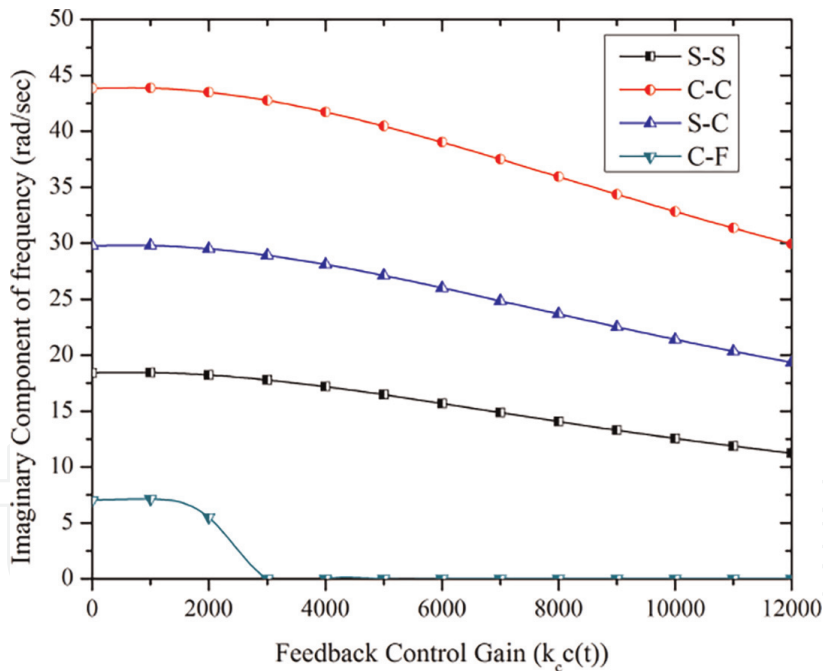
Figure 13.
Variation of imaginary component of the frequency with changes in feedback control gain at $r = 0.005$ m and $v = 5$ m/s.

frequency of FGMT fluid conveying pipe calculated based on relations published by [38] for simply supported boundary condition. It has been shown that when fluid velocity rises, the nonlinear frequency falls.

Figure 16 depicts the coupled effect of feedback control gain along with thermal loading. It is inferred that, there is decreasing effect of critical flow velocity as thermal loading increases. The reduction in overall stiffness of pipe is the reason for instability of FGMT pipe at lower flow velocity with thermal loading. Therefore, critical flow
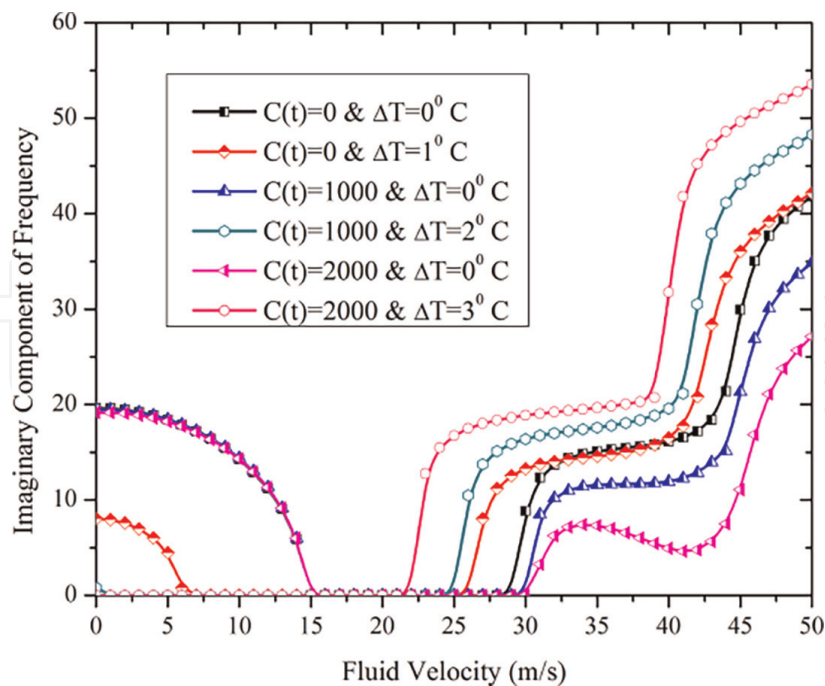
Figure 14.
Variation of clamped-free fundamental frequency with changes in control gain and fluid velocity.

Figure 15.
Variation of nonlinear simply supported frequency with changes in fluid velocity.

velocity condition under thermal loading can be amplified through imposing higher feedback control gain. The control gain varies between 0 and 2000 as the temperature of the fluid conveying pipe changes. It is inferred that, with a zero control gain and 1°C and 0°C, the instability state of the fluid conveying pipe reduces from a fluid velocity from 27 to 25.2 m/s. Additionally, with a control gain of 1000, the fluid conveying pipe's unstable condition decreases from 29 to 24 m/s. Similar to this, with the control gain of 2000, the fluid conveying pipe's unstable condition decreases from 30 to 22 m/s.

Figure 16.
Variation of S-S fundamental frequency with changes in control gain, thermal loading and fluid velocity.

6. Concluding remarks

In this chapter, the differential quadrature and differential transform method is applied to analyze the free vibration of FGMT pipes conveying fluid with different boundary conditions. Boundary value problem of FGMT fluid-conveying pipe is solved straightforwardly using DQM and DTM. Close agreement is established for critical velocity and frequencies results generated by DQM, DTM with those of Navier and Galerkin solution. Eigenvalue diagrams are detailed enough to shows the illustration about the effects of feedback control gain, density of fluid, inner radius of pipe and thermal loading on the vibrational and instability characteristics. To attenuate the amplitude of vibration or displacement, inherent damping property of the material cannot be sufficient. To dampen out large amplitude vibration during resonance, special techniques have been explored, like using sandwich pipes namely, viscoelastic layer placed between two layers of the parent pipe material. This approach is called passive damping. Viscoelastic materials like, natural rubber, and synthetic rubber like nitrile butadine rubber and styrene butadine rubber, silicone rubber can be proposed. Sophisticated technique is the active vibration. This method involves use of materials like, piezoelectric, magnetostrictive, magnetorehology, electrostricitve and shape memory alloys. Magnetostrictive material presented in this chapter works on the ability of the material to respond mechanically to the presence of magnetic field. The magnetic field is produced using a coil with passage of time dependent current. A magnetostrictive material responds with a force, hence magnetostrictive actuator. The force produced should be used to counteract the forces due to vibration. Thus, damping is introduced. The idea of incorporting Terfenol-D layer facilitates the best control of the fluid conveying FGMT pipe to avoid the bifurcation and flutter instabilities and achieve more adaptive and efficient system. Additionally increasing or decreasing effect of feedback control gain and thermal loading on critical flow velocity and instabilities have been addressed.

Conflict of interest

The authors declare no conflict of interest.

Abbreviations

FGMT   Functionally graded material integrated with Terfenol-D
BC   boundary conditions
DQM   differential quadrature method
DTM   differential transform method
ODE   ordinary differential equation

Author details

Mukund A. Patil[1†] and Ravikiran Kadoli[2*†]

1 Department of Mechanical Engineering, G.H. Raisoni Institute of Engineering and Business Management, Jalgaon, Maharashtra, India

2 Department of Mechanical Engineering, National Institute of Technology Karnataka, Surathkal, Mangalore, Karnataka, India

*Address all correspondence to: rkkadoli@nitk.edu.in

† These authors contributed equally.

IntechOpen

References

[1] Tijsseling AS. Fluid-structure interaction in liquid-filled pipe systems: A review. Journal of Fluids and Structures. 1996;**10**(2):109-146

[2] Ibrahim RA. Overview of mechanics of pipes conveying fluids—Part I: Fundamental studies. Journal of Pressure Vessel Technology. 2010;**132**(3):034001-1-32

[3] Ibrahim RA. Mechanics of pipes conveying fluids—part ii: Applications and fluidelastic problems. Journal of Pressure Vessel Technology. 2011;**133**(2):024001-1-30

[4] Li S, Karney BW, Liu G. Fsi research in pipeline systems–a review of the literature. Journal of Fluids and Structures. 2015;**57**:277-297

[5] Chen S-S. Free vibration of a coupled fluid/structural system. Journal of Sound and Vibration. 1972;**21**(4):387-398

[6] Zhai H-b, Zi-yan W, Liu Y-s, Yue Z-f. Dynamic response of pipeline conveying fluid to random excitation. Nuclear Engineering and Design. 2011;**241**(8):2744-2749

[7] Cigeroglu E, Samandari H. Nonlinear free vibrations of curved double walled carbon nanotubes using differential quadrature method. Physica E: Low-dimensional Systems and Nanostructures. 2014;**64**:95-105

[8] Tang Y, Yang T. Post-buckling behavior and nonlinear vibration analysis of a fluid-conveying pipe composed of functionally graded material. Composite Structures. 2018;**185**:393-400

[9] Li B, Wang Z, Jing L. Dynamic response of pipe conveying fluid with lateral moving supports. Shock and Vibration. 2018;**2018**:1-17

[10] Wang Y, Zhang Q, Wang W, Yang T. In-plane dynamics of a fluid-conveying corrugated pipe supported at both ends. Applied Mathematics and Mechanics. 2019;**40**(8):1119-1134

[11] Ni Q, Zhang ZL, Wang L. Application of the differential transformation method to vibration analysis of pipes conveying fluid. Applied Mathematics and Computation. 2011;**217**(16):7028-7038

[12] Li Y-d, Yang Y-r. Forced vibration of pipe conveying fluid by the green function method. Archive of Applied Mechanics. 2014;**84**(12):1811-1823

[13] Dai HL, Wang L. Dynamics and stability of magnetically actuated pipes conveying fluid. International Journal of Structural Stability and Dynamics. 2016;**16**(06):1550026

[14] Oke WA, Khulief YA. Effect of internal surface damage on vibration behavior of a composite pipe conveying fluid. Composite Structures. 2018;**194**:104-118

[15] Sutar S, Madabhushi R, Chellapilla KR, Poosa RB. Determination of natural frequencies of fluid conveying pipes using muller's method. Journal of The Institution of Engineers (India): Series C. 2019;**100**(3):449-454

[16] Rafiee R, Sharifi P. Stochastic failure analysis of composite pipes subjected to random excitation. Construction and Building Materials. 2019;**224**:950-961

[17] Rajidi SR, Gupta A, Panda S. Vibration characteristics of viscoelastic sandwich tube conveying fluid. Materials Today: Proceedings. 2020;**28**:2440-2446

[18] Amiri A, Masoumi A, Talebitooti R. Flutter and bifurcation instability analysis of fluid-conveying micro-pipes sandwiched by magnetostrictive smart layers under thermal and magnetic field. International Journal of Mechanics and Materials in Design. 2020;**16**(3):569-588

[19] Soltani P, Bahar P, Farshidianfar A. An efficient gdq model for vibration analysis of a multiwall carbon nanotube on pasternak foundation with general boundary conditions. Proceedings of the Institution of Mechanical Engineers, Part C: Journal of Mechanical Engineering Science. 2011;**225**(7):1730-1741

[20] Bahaadini R, Hosseini M. Effects of nonlocal elasticity and slip condition on vibration and stability analysis of viscoelastic cantilever carbon nanotubes conveying fluid. Computational Materials Science. 2016;**114**:151-159

[21] Askari H, Esmailzadeh E. Forced vibration of fluid conveying carbon nanotubes considering thermal effect and nonlinear foundations. Composites Part B: Engineering. 2017;**113**:31-43

[22] Kamali M, Mohamadhashemi V, Jalali A. Parametric excitation analysis of a piezoelectric-nanotube conveying fluid under multi-physics field. Microsystem Technologies. 2018;**24**(7):2871-2885

[23] Liang F, Yang XD, Bao RD, Zhang W. Frequency analysis of functionally graded curved pipes conveying fluid. Advances in Materials Science and Engineering. 2016;**2016**:1-9

[24] Zhou X-w, Dai H-L, Wang L. Dynamics of axially functionally graded cantilevered pipes conveying fluid. Composite Structures. 2018;**190**:112-118

[25] Dai J, Liu Y, Liu H, Miao C, Tong G. A parametric study on thermo-mechanical vibration of axially

functionally graded material pipe conveying fluid. International Journal of Mechanics and Materials in Design. 2019;**15**(4):715-726

[26] Heshmati M. Influence of an eccentricity imperfection on the stability and vibration behavior of fluid-conveying functionally graded pipes. Ocean Engineering. 2020;**203**:107192

[27] Liang X, Zha X, Jiang X, Wang L, Leng J, Cao Z. Semi-analytical solution for dynamic behavior of a fluid-conveying pipe with different boundary conditions. Ocean Engineering. 2018;**163**:183-190

[28] Yi-min H, Ge Seng W, Wei, and He Jie. A direct method of natural frequency analysis on pipeline conveying fluid with both ends supported. Nuclear Engineering and Design. 2012;**253**:12-22

[29] Łuczko J, Czerwiński A. Three-dimensional dynamics of curved pipes conveying fluid. Journal of Fluids and Structures. 2019;**91**:102704

[30] Engdahl G, Mayergoyz ID. Handbook of Giant Magnetostrictive Materials. Vol. 386. San Diego: Academic Press; 2000

[31] Patil MA, Kadoli R. Differential quadrature solution for vibration control of functionally graded beams with terfenol-d layer. Applied Mathematical Modelling. 2020;**84**:137-157

[32] Reddy JN, Barbosa JI. On vibration suppression of magnetostrictive beams. Smart Materials and Structures. 2000;**9**(1):49-58

[33] Qian Q, Wang L, Ni Q. Instability of simply supported pipes conveying fluid under thermal loads. Mechanics Research Communications. Apr 2009;**36**(3):413-417

[34] Lin W, Qiao N. In-plane vibration analyses of curved pipes conveying fluid using the generalized differential quadrature rule. Computers & Structures. 2008;**86**(1–2):133-139

[35] Talebitooti M, Fadaee M. A magnetostrictive active vibration control approach for rotating functionally graded carbon nanotube-reinforced sandwich composite beam. Smart Materials and Structures. 2019;**28**(7): 075007

[36] Patil MA, Kadoli R. Effect of two-parameter partial foundation and viscoelastic supports on free vibration of Terfenol-D layered functionally graded fluid conveying pipe using domain decomposition technique. Mechanics of Advanced Materials and Structures. 2022:1-13. DOI: 10.1080/15376494.2022. 2103604

[37] Li Li, Yujin Hu. Critical flow velocity of fluid-conveying magneto-electro-elastic pipe resting on an elastic foundation. International Journal of Mechanical Sciences. Dec 2016;**119**: 273-282

[38] Shamim M, Mehran S, Davood Y, Ebrahim E. Nonlinear vibration analysis of fluid-conveying microtubes. Nonlinear Dynamic. Mar 2016; **85**(2): 1007-1021